State feedback control and observer-based adaptive synchronisation of chaos in a memristive Murali–Lakshmanan–Chua circuit

A ISHAQ AHAMED[1] and M LAKSHMANAN[2] [iD],*

[1]Department of Physics, Jamal Mohamed College (Affiliated to Bharathidasan University), Tiruchirappalli 620 020, India
[2]Department of Nonlinear Dynamics, School of Physics, Bharathidasan University, Tiruchirappalli 620 024, India
*Corresponding author. E-mail: lakshman.cnld@gmail.com

Abstract. In this paper we report the control and synchronisation of chaos in a memristive Murali–Lakshmanan–Chua (MLC) circuit. This circuit, introduced by the present authors in 2013, is basically a non-smooth system having two discontinuity boundaries by virtue of it having a flux-controlled active memristor as its nonlinear element. While the control of chaos has been effected using state feedback techniques, the concept of adaptive synchronisation and observer-based approaches have been used to effect synchronisation of chaos. Both these techniques are based on state space representation theory which is well known in the field of control engineering. As in our earlier works on this circuit, we have derived the Poincaré discontinuity mapping (PDM) and zero time discontinuity mapping (ZDM) corrections, both of which are essential for realising the true dynamics of non-smooth systems. Further, we have constructed the observer- and controller-based canonical forms of the state-space representations, have set up the Luenberger observer, derived the controller gain vector to implement state feedback control and calculated the gain matrices for switch feed back and finally performed parameter estimation for effecting observer-based adaptive synchronisation. Our results obtained by numerical simulation include time plots, phase portraits, estimation of the parameters and convergence of error graphs and phase plots showing complete synchronisation.

Keywords. Memristive Murali–Lakshmanan–Chua circuit; state-space representations; canonical forms; Luenberger observer; feedback control; gain vectors and matrices; pole placement.

PACS Nos 12.60.Jv; 12.10.Dm; 98.80.Cq; 11.30.Hv

1. Introduction

Chaotic systems are characterised by their high sensitivity to even infinitesimal changes in their initial conditions. As a result, these systems, by their intrinsic nature, defy attempts at control or synchronisation. Nevertheless, many techniques have been proposed by a large group of researchers to control and synchronise chaotic systems. Control of chaos refers to a process wherein a judiciously chosen perturbation is applied to a chaotic system, in order to realise a desirable behaviour [1]. Since the seminal contribution by Ott *et al* in 1990 [2], the concept of control of chaos has been modified and developed by many researchers [3] and applied to a large number of physical systems [4]. Synchronisation of chaos, on the other hand, can be described as a process wherein two or more chaotic systems (either

equivalent or non-equivalent) adjust a given property of their motion to a common behaviour, due to coupling or forcing. This may range from complete agreement of trajectories to locking of phases [5–7].

In this paper, we describe the general principles of control of chaos using state feedback mechanism and synchronisation of chaotic systems using observer-based adaptive techniques. Further using these, we report the control of chaos in a single memristive Murali–Lakshmanan–Chua (MLC) oscillator and the synchronisation of chaos in a two-coupled memristive MLC oscillator system. The paper is organised as follows. In §2 we give a brief introduction of the memristive MLC circuit, its circuit realisation, its circuit equations and their normalised forms and the description of the circuit as a non-smooth system. In §3 the various algorithms for the control of chaos are outlined. In §4 the
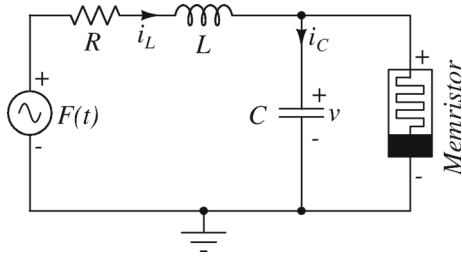
Figure 1. The memristive MLC circuit.

control of chaos in the memristive MLC circuit using state feedback control technique is dealt with. Similarly, in §§5 and 6 the concept of synchronisation of chaos and its realisation are explained, while in §7 the observer-based adaptive synchronisation of chaos in a system of two-coupled memristive MLC oscillator is described. Finally in §8, the results and further discussions are given.

2. Memristive Murali–Lakshmanan–Chua circuit

The memristive MLC circuit was introduced by the present authors [8] by replacing the Chua's diode in the classical Murali–Lakshmanan–Chua circuit with an active flux-controlled memristor as its non-linear element. The analog model of the memristor used in this work was designed by Ishaq Ahamed *et al* [9]. The schematic of the memristive MLC circuit is shown in figure 1, while the actual analog realisation based on the prototype model for the memristor is shown in figure 2.

Applying Kirchoff's laws, the circuit equations can be written as a set of autonomous ordinary differential equations (ODEs) for the flux $\phi(t)$, voltage $v(t)$, current $i(t)$ and the time p in the extended coordinate system as

$$\frac{\mathrm{d}\phi}{\mathrm{d}t} = v,$$
$$C\frac{\mathrm{d}v}{\mathrm{d}t} = i - W(\phi)v,$$
$$L\frac{\mathrm{d}i}{\mathrm{d}t} = -v - Ri + F\sin(\Omega p),$$
$$\frac{\mathrm{d}p}{\mathrm{d}t} = 1. \tag{1}$$

Here $W(\phi)$ is the memductance of the memristor and is as defined in [10] as

$$W(\phi) = \frac{\mathrm{d}q(\phi)}{\mathrm{d}\phi} = \begin{cases} G_{a_1}, & |\phi| > 1, \\ G_{a_2}, & |\phi| \le 1, \end{cases} \tag{2}$$

where G_{a_1} and G_{a_2} are respectively the slopes of the outer and inner segments of the characteristic curve of

the memristor. We can rewrite eqs (1) in the normalised form as

$$\dot{x}_1 = x_2,$$
$$\dot{x}_2 = x_3 - W(x_1)x_2,$$
$$\dot{x}_3 = -\beta(x_2 + x_3) + f\sin(\omega x_4),$$
$$\dot{x}_4 = 1. \tag{3}$$

Here dot stands for differentiation with respect to the normalised time τ (see below) and $W(x_1)$ is the normalised value of the memductance of the memristor, given as

$$W(x_1) = \frac{\mathrm{d}q(x_1)}{\mathrm{d}x_1} = \begin{cases} a_1, & |x_1| > 1, \\ a_2, & |x_1| \le 1, \end{cases} \tag{4}$$

where $a_1 = G_{a_1}/G$ and $a_2 = G_{a_2}/G$ are the normalised values of G_{a_1} and G_{a_2} mentioned earlier and are negative. The rescaling parameters used for the normalisation are

$$x_1 = \frac{G\phi}{C}, \; x_2 = v, \; x_3 = \frac{i}{G}, \; x_4 = \frac{Gp}{C}, \; G = \frac{1}{R},$$
$$\beta = \frac{C}{LG^2}, \; \omega = \frac{\Omega C}{G} = \frac{2\pi\nu C}{G}, \; \tau = \frac{Gt}{C}, \; f = F\beta. \tag{5}$$

In our earlier work on this memristive MLC circuit, see [8], we reported that the addition of memristor as the nonlinear element converts the system into a piecewise-smooth continuous flow having two discontinuous boundaries, admitting 'grazing bifurcations', a type of discontinuity induced bifurcation (DIB). These grazing bifurcations were identified as the cause for the occurrence of hyperchaos, hyperchaotic beats and transient hyperchaos in this memristive MLC system. Further we have reported 'discontinuity-induced Hopf and Neimark–Sacker bifurcations' in the same circuit, refer [11]. Thus, the memristive MLC circuit shows rich dynamics by virtue of it being a non-smooth system. Hence, we give a brief description of the memristive MLC circuit in the framework of non-smooth bifurcation theory.

2.1 *Memristive MLC circuit as a non-smooth system*

The memristive MLC circuit is a piecewise-smooth continuous system by virtue of the discontinuous nature of its nonlinearity, namely the memristor. An active flux-controlled memristor is known to switch state with respect to time from a more conductive ON state to a less conductive OFF state and vice versa at some fixed values of flux across it, see [11]. In the normalised coordinates, this switching is found to occur at $x_1 = +1$ and $x_1 = -1$. These switching states of
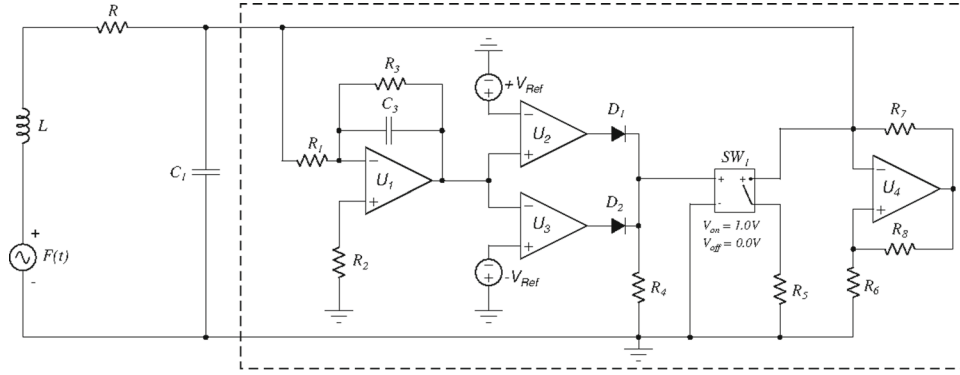
Figure 2. A multisim prototype model of a memristive MLC circuit. The memristor part is shown by the dashed outline. The parameter values of the circuit are fixed as $L = 21$ mH, $R = 900\,\Omega$, $C_1 = 10.5$ nF. The frequency of the external sinusoidal forcing is fixed as $\nu_{\text{ext}} = 8.288$ kHz and the amplitude is fixed as $F = 770$ mV$_{\text{pp}}$ (peak-to-peak voltage).

the memristor give rise to two discontinuity boundaries or switching manifolds, $\Sigma_{1,2}$ and $\Sigma_{2,3}$, which are symmetric about the origin and are defined by the zero sets of the smooth functions $H_i(\mathbf{x}, \mu) = C^T\mathbf{x}$, where $C^T = [1, 0, 0, 0]$ and $\mathbf{x} = [x_1, x_2, x_3, x_4]$, for $i = 1, 2$. Hence, $H_1(\mathbf{x}, \mu) = (x_1 - x_1^*)$, $x_1^* = -1$ and $H_2(\mathbf{x}, \mu) = (x_1 - x_1^*)$, $x_1^* = +1$, respectively. Consequently, the phase space $\mathcal{D}$ can be divided into three subspaces S_1, S_2 and S_3 due to the presence of the two switching manifolds. The memristive MLC circuit can now be rewritten as a set of smooth ODEs
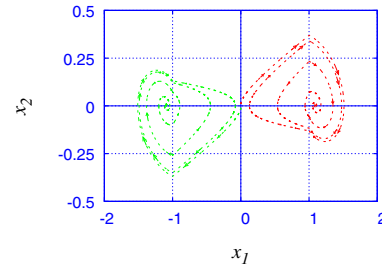

Figure 3. The equilibrium points $E_\pm$ in the subspaces S_1 and S_3 for the parameter value above $\beta_c = 0.8250$. The initial conditions are $x_1 = 0.0$, $x_2 = 0.01$, $x_3 = 0.01$ for the fixed point E_+ in the subspace S_3 and $x_1 = 0.0$, $x_2 = -0.01$, $x_3 = -0.01$ for the fixed point E_- in the subspace S_1.

$$\dot{x}(t) = \begin{cases} F_{1,3}(\mathbf{x}, \mu), & H_1(\mathbf{x}, \mu) < 0 \text{ and } H_2(\mathbf{x}, \mu) > 0, \ \mathbf{x} \in S_{1,3} \\ F_2(\mathbf{x}, \mu), & H_1(\mathbf{x}, \mu) > 0 \text{ and } H_2(\mathbf{x}, \mu) < 0, \ \mathbf{x} \in S_2 \end{cases} \tag{6}$$

where μ denotes the parameter dependence of the vector fields and the scalar functions. The vector fields F_i's are

$$F_i(\mathbf{x}, \mu) = \begin{pmatrix} x_2 \\ -a_i x_2 + x_3 \\ -\beta x_2 - \beta x_3 + f \sin(\omega x_4) \\ 1 \end{pmatrix},$$

$$i = 1, 2, 3, \tag{7}$$

where we have $a_1 = a_3$.

The discontinuity boundaries $\Sigma_{1,2}$ and $\Sigma_{2,3}$ are not uniformly discontinuous. This means that the degree of smoothness of the system in some domain $\mathcal{D}$ of the boundary is not the same for all points $x \in \Sigma_{ij} \cap \mathcal{D}$. This causes the memristive MLC circuit to behave as a non-smooth system having a degree of smoothness of either one or two. In such a case, it will behave either as a 'Filippov system' or as a 'piecewise-smooth continuous flow' respectively, refer Appendix A in [11].

2.2 *Equilibrium points and their stability*

In the absence of the driving force, that is if $f = 0$, the memristive MLC circuit can be considered as a three-dimensional autonomous system with vector fields given by

$$F_i(\mathbf{x}, \mu) = \begin{pmatrix} x_2 \\ -a_i x_2 + x_3 \\ -\beta x_2 - \beta x_3 \end{pmatrix}, \quad i = 1, 2, 3. \tag{8}$$

This three-dimensional autonomous system has a trivial equilibrium point E_0, two 'admissible equilibrium' points $E_\pm$ and two 'boundary equilibrium' points $E_{B\pm}$. The trivial equilibrium point is given as

$$E_0 = \{(x_1, x_2, x_3) | x_1 = x_2 = x_3 = 0\}. \tag{9}$$

The two admissible equilibria $E_\pm$ are

$$E_\pm = \{(x_1, x_2, x_3) | x_2 = x_3 = 0, x_1^*$$
$$= \text{constant and not equal to} \pm 1\}. \tag{10}$$

The two boundary equilibrium points are

$$E_{B\pm} = \{(x_1, x_2, x_3) | x_2 = x_3 = 0, \hat{x}_1 = \pm 1\}. \quad (11)$$

The multiplicity of equilibrium points arises because of the non-smooth nature of the nonlinear function, namely $W(x_1)$ given in eq. (4). To find the stability of these equilibrium states, we construct the Jacobian matrices N_i, $i = 1, 2, 3$ and evaluate their eigenvalues at these points,

$$N_i = \begin{pmatrix} 0 & 1 & 0 \\ 0 & -a_i & 1 \\ 0 & -\beta & -\beta \end{pmatrix}, \quad i = 1, 2, 3. \quad (12)$$

The characteristic equation associated with system N_i in these equilibrium states is

$$\lambda^3 + p_2\lambda^2 + p_1\lambda = 0, \quad (13)$$

where λ's are the eigenvalues that characterise the equilibrium states and p_i's are the coefficients, given as $p_1 = \beta(1 + a_i)$ and $p_2 = (\beta + a_i)$. The eigenvalues are

$$\lambda_1 = 0, \quad \lambda_{2,3} = \frac{-(\beta + a_i)}{2} \pm \frac{\sqrt{(\beta - a_i)^2 - 4\beta}}{2}, \quad (14)$$

where $i = 1, 2, 3$. Depending on the eigenvalues, the nature of the equilibrium states differ.

1. When $(\beta - a_i)^2 = 4\beta$, the equilibrium state will be a stable/unstable star depending on whether $(\beta + a_i)$ is positive or not.
2. When $(\beta - a_i)^2 > 4\beta$, the equilibrium state will be a saddle.
3. When $(\beta - a_i)^2 < 4\beta$, the equilibrium state will be a stable/unstable focus.

For the third case, the circuit admits self-oscillations with natural frequency varying in the range

$$\sqrt{[(\beta - a_1)^2 - 4\beta]}/2 < \omega_0 < \sqrt{[(\beta - a_2)^2 - 4\beta]}/2.$$

It is at this range of frequency that the memristor switching also occurs.

As the vector fields $F_1(\mathbf{x}, \mu)$ and $F_3(\mathbf{x}, \mu)$ are symmetric about the origin, that is $F_1(\mathbf{x}, \mu) = F_3(-\mathbf{x}, \mu)$, the admissible equilibria $E_\pm$ are also placed symmetric about the origin in the subspaces S_1 and S_3. These are shown in figure 3 for a certain choice of parametric values.

2.3 *Sliding bifurcations and chaos*

Let us assume the bifurcation points at the two switching manifolds to be

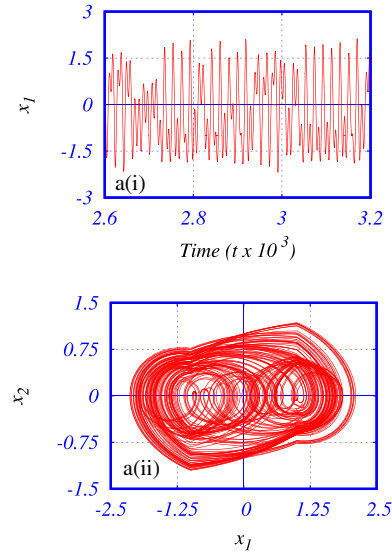$$E_{B\pm} = \{(x_1, x_2, x_3) | x_2 \neq 0, x_3 = 0, \hat{x}_1 = \pm 1\}. \quad (15)$$

Figure 4. The chaotic dynamics of the memristive MLC oscillator arising due to sliding bifurcations occurring in the circuit, with **a(i)** the time plot of the x_1 variable and **a(ii)** phase portrait in the (x_1–x_2) plane. The step size is assumed as $h = \frac{1}{1000}(2\pi/\omega)$, with $\omega = 0.65$ and $f = 0.20$.

Then we find from eqs (8) that $F_2(x, \mu) \neq F_1(x, \mu)$ at $x \in \Sigma_{1,2}$ and $F_2(x, \mu) \neq F_3(x, \mu)$ at $x \in \Sigma_{2,3}$. Under such conditions, the system is said to have a degree of smoothness of order 'one', that is $r = 1$. Hence, the memristive MLC circuit can be considered to behave as a Filippov system or a Filippov flow capable of exhibiting sliding bifurcations.

Sliding bifurcations are discontinuity-induced bifurcations (DIBs) arising due to the interactions between the limit cycles of a Filippov system with the boundary of a sliding region. Four types of sliding bifurcations have been identified by Feigin [12] and were subsequently analysed by di Bernado, Kowalczyk and others [13–16] for a general n-dimensional system. These four sliding bifurcations are crossing-sliding bifurcations, grazing-sliding bifurcations, switching-sliding bifurcations and adding-sliding bifurcations.

The memristive MLC circuit is found to admit three types of sliding bifurcations, namely crossing-sliding, grazing-sliding and switching sliding bifurcations [17]. Let the parameters be chosen as $a_{1,3} = -0.55$, $a_2 = -1.02$, $\beta = 0.95$, $f = 0.20$ and $\omega = 0.65$. For these parameters, the memristive MLC circuit undergoes repeated sliding bifurcations at the discontinuity boundaries $\Sigma_{1,2}$ and $\Sigma_{2,3}$, giving rise to a chaotic state as shown in figure 4. Here a(i) shows the time plot of the x_1 variable and a(ii) shows the phase portrait in the (x_1–x_2) plane. In the subsequent section, we shall show

that this chaotic behaviour exhibited by the memristive MLC circuit can be controlled using state feedback control technique.

3. Control of chaos

Control of chaos refers to purposeful manipulation of the chaotic behaviour of a nonlinear system to some desired or preferred dynamical state. As chaotic behaviour is considered undesired or harmful, a need was felt for suppression of chaos or at least reducing it as much as possible. For example, control of chaos is necessary in avoiding fatal voltage collapses in power grids, elimination of cardiac arrhythmias, guiding cellular neural networks to reach certain desirable pattern formations, etc. The earliest attempts at controlling chaos were focussed on eliminating the response of a chaotic system, which resulted in the destruction of the dynamics of the system itself. However, it was Ott *et al* [2] who showed that it would be beneficial to force the chaotic system to one of its infinite unstable periodic orbits (UPO) which are embedded in the chaotic attractor of the system without totally destroying the dynamics of the system. Following this, many workers have developed newer techniques to control chaos and have applied them successfully on a variety of systems to realise different desired behaviours. Generally, all the known methods of chaos control can be grouped into two categories, either feedback control methods or non-feedback control algorithms.

3.1 *Feedback controlling algorithms*

Feedback control algorithms essentially make use of the intrinsic properties of chaotic systems to stabilise orbits which are already existing in the systems. The adaptive control algorithm (ACA) developed by Huberman and Lumer [18] and applied by Sinha *et al* [19] and Rajasekar and Lakshmanan [3], the Ott–Grebogi–Yorke (OGY) algorithm developed by Ott *et* al [2] and applied in [5, 20–23], the control engineering approach, developed in [24,25] are all examples of these algorithms.

3.2 *Non-feedback methods*

The non-feedback methods refer to the use of some small perturbing external force, or noise, or a constant bias potential, or a weak modulating signal to some system parameter. The parametric control of chaos was demonstrated in [3,5,26–30]. The control

of chaos by applying a constant weak biasing voltage was demonstrated in [5] in the case of MLC oscillator and Duffing oscillator and by the addition of noise was demonstrated in a BVP oscillator in [3]. The other control algorithms are entrainment or open loop control method developed and applied in [31–35] and the oscillation absorber method developed in [36,37].

3.3 *Control of chaos using state feedback*

As the feedback and non-feedback methods of chaos control have many drawbacks, a continuous time feedback control using small perturbations was proposed numerically by Pyragas [38]. This control scheme was provided a rigorous basis by Chen and Dong and was demonstrated successfully in time continuous systems like Duffing oscillator [39], Chua's circuit [25,40] and so on. However, the drawbacks of these methods are

1. they can be applied only when the dynamical equations for the system are known *a priori*
2. the internal state variables are assumed to be available to construct control forces
3. the controller structure, in some cases, is extremely complicated
4. limited information may be available and the only measurable quantity of the system is its output
5. for non-smooth systems, these conventional techniques, in particular addition of a second weak periodic excitation or the addition of a constant bias do not seem to enforce control of chaos

Under such conditions, a parallel state reconstruction by means of either a Kalman filter or Luenberger-type observer must be used to implement control laws. For this purpose, the state-space representation of the system and their transformations to either controller canonical form or observer canonaical form are derived, refer Appendix A.

The state-space representation refers to the modelling of dynamical systems in terms of state vectors and matrices so that the analyses of such systems are made conveniently in the time domain, using the basic knowledge of matrix algebra [41,42]. This representation is a well researched area in the field of control engineering [41,43,44]. The main advantage of this approach is that it presents a uniform platform for representing time-varying as well as time-invariant systems, linear as well as piece-wise nonlinear systems. Further, the vector fields for all the subspaces of the system take on a uniform form. Some of the methods of control that fall in this category are adaptive control

[45], observer-based control [46], sliding mode control [47], impulsive control [48] and backstepping control [49], linear switched state feedback method [50], twin-T notch filter method [51] and backstepping method [52].

In this section, we outline the feedback method for the control of chaos in a general dynamical system using state-space models. Let us consider the observer canonical representation of a single input single output (SISO) nonlinear chaotic system in state space, refer eq. (A.9) in Appendix A,

$$\dot{x}_0 = \tilde{A}x_0 + B^T u,$$
$$y = C_0^T x_0 + D^T u, \tag{16}$$

where $\tilde{A} \in \mathcal{R}^{n \times n}$, $B \in \mathcal{R}^{n \times r}$, $C \in \mathcal{R}^{n \times l}$ and $D \in \mathcal{R}^{l \times r}$ are matrices, u is an r-dimensional vector denoting the control input and y is an l-dimensional vector representing the output of the system. This system is often called as the 'open-loop system' in control theory.

Being in the observer canonical form, the system matrix $\tilde{A}$ is given as

$$\tilde{A} = \begin{pmatrix} -\tilde{a}_1 & 1 & 0 & \cdots & 0 \\ -\tilde{a}_2 & 0 & 1 & \cdots & 0 \\ \vdots & \vdots & \vdots & \cdots & \vdots \\ -\tilde{a}_{n-1} & 0 & 0 & \cdots & 1 \\ -\tilde{a}_n & 0 & 0 & \cdots & 0 \end{pmatrix}, \tag{17}$$

where $\tilde{a}_i$'s are the coefficients of the characteristic polynomial $\{|sI - \tilde{A}|\}$.

If we want the states of the system to approach zero starting from any arbitrary state, then we have to design a control input which would regulate the states of the system to the desired equilibrium conditions. To achieve this, we assume a 'state feedback control law'

$$u = -\tilde{K}x_0, \tag{18}$$

where $\tilde{K}$ is called the 'control gain vector' and can be designed using pole placement technique, familiar in control theory.

Substituting this control law, eq. (18) in the state-space representation of the open-loop system, eq. (16), the system now becomes a 'closed-loop system' represented as

$$\dot{x}_0 = (\tilde{A} - B^T \tilde{K})x_0,$$
$$y = C_0^T x_0 + D^T u, \tag{19}$$

where B^T is the transpose of the vector B and the closed-loop system matrix is given as

$$(\tilde{A} - B^T \tilde{K}) = \begin{pmatrix} -(\tilde{a}_1 - \tilde{k}_n) & 1 & 0 & \cdots & 0 \\ -(\tilde{a}_2 - \tilde{k}_{n-1}) & 0 & 1 & \cdots & 0 \\ \vdots & & \vdots & \vdots & \cdots & \vdots \\ -(\tilde{a}_{n-1} - \tilde{k}_2) & 0 & 0 & \cdots & 1 \\ -(\tilde{a}_n - \tilde{k}_1) & 0 & 0 & \cdots & 0 \end{pmatrix}. \tag{20}$$

If the values of $\tilde{K}$ are so chosen that the eigenvalues of the matrix $(\tilde{A} - B^T \tilde{K})$ lie within the unit circle in the complex plane, then the system can be controlled to a desired stable equilibrium state. The problem of chaos control thus reduces to just determining a state feedback control gain vector $\tilde{K}$ such that the control law, eq. (18), places the poles of the closed-loop system, eq. (19), in the desired locations. An illustration of this concept is shown in the block diagram in figure 5.

A necessary and sufficient condition for the successful pole placement is that the nonlinear system, that is, the pair of matrices $(\tilde{A}, B)$, must be controllable.

Let the characteristic polynomial $\{sI - (\tilde{A} - B^T \tilde{K})\}$ of the closed-loop system, eq. (19), be given as

$$s^n + (\tilde{a}_1 - \tilde{k}_n)s^{n-1} + (\tilde{a}_2 - \tilde{k}_{n-1})s^{n-2}$$
$$+ \cdots + (\tilde{a}_n - \tilde{k}_1) = 0. \tag{21}$$

Let the characteristic equation of the desired control state of the system be

$$(s - s_1)(s - s_2)(s - s_3) \cdots (s - s_n) = 0,$$
$$s^n + \alpha_1 s^{n-1} + \alpha_2 s^{n-2} + \cdots + \alpha_{n-1}s + \alpha_n = 0, \tag{22}$$

where $s_i, i = 1, 2, \ldots, n$ are the desired poles to which the system should be guided and $\alpha_i, i = 1, 2, \ldots, n$ are the coefficients of the desired characteristic equation. By comparing eqs (21) and (22), we get the elements of the transformed control gain vector $\tilde{K}$ as

$$\tilde{k}_n = \alpha_1 - \tilde{a}_1,$$
$$\tilde{k}_{n-1} = \alpha_2 - \tilde{a}_2,$$
$$\tilde{k}_{n-3} = \alpha_3 - \tilde{a}_3, \ldots,$$
$$\tilde{k}_1 = \alpha_n - \tilde{a}_n.$$

4. Control of chaos in memristive MLC circuit

In the earlier sections, we have seen that the memristive MLC circuit is a piecewise-smooth dynamical system having two discontinuity boundaries causing the state space of the system to be split up into three subspaces. Consequently, the memristive MLC circuit is
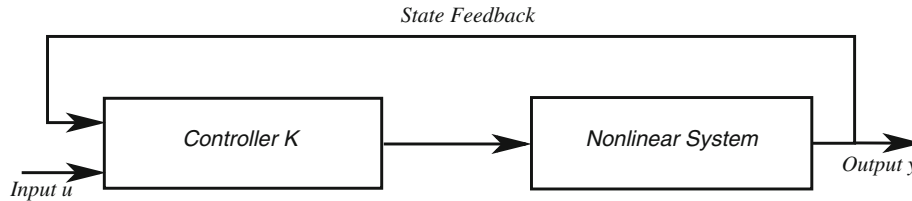
Figure 5. Block diagram illustrating the concept of state feedback control.

represented by a set of smooth ODE's, refer eqs (6). Further, we have seen that for the boundary equilibrium points given by eqs (15), the memristive MLC circuit becomes a Filippov system.

Linearising the vector fields about the equilibrium points defined by eqs (15), the observer canonical form of the state-space representation of the memristive MLC oscillator as a SISO system, refer eq. (A.9) in Appendix A, can be given as

$$\dot{x}_0(t) = \begin{cases} \tilde{A}_2 x_0 + B^T u & \text{if } x \in S_2, \\ \tilde{A}_{1,3} x_0 + B^T u & \text{if } x \in S_{1,3}, \end{cases}$$
$$y = C^T x + D^T u, \tag{23}$$

where the system matrices $\tilde{A}_i$'s are calculated for the above chosen parameters as

$$\tilde{A}_2(x) = \begin{pmatrix} 0.0700 & 1.0 & 0.0 \\ 0.0190 & 0.0 & 1.0 \\ 0.0000 & 0.0 & 0.0 \end{pmatrix}, \tag{24}$$

while

$$\tilde{A}_{1,3}(x) = \begin{pmatrix} -0.4000 & 1.0 & 0.0 \\ -0.4275 & 0.0 & 1.0 \\ -0.0000 & 0.0 & 0.0 \end{pmatrix}. \tag{25}$$

Further, the vectors B^T, C^T and D^T are chosen as

$$B^T = (0\ 1\ 0), \tag{26}$$
$$C^T = (1\ 0\ 0), \tag{27}$$
$$D^T = (0\ 0\ 0). \tag{28}$$

We assume here that no disturbance is present in the system, that is, the vector D^T is a null vector $D = 0$.

The peculiarity of this observer canonical representation, eqs (23), is that the transformations required become identical for all the three subregions of the phase space. This is particularly helpful in studying nonsmooth bifurcations of piecewise-smooth systems [53].

The controllability matrices for the subspaces $S_{1,3}$ for the aforementioned parameters are given as

$$P_{c1,3} = \begin{pmatrix} 0.0 & 1.00 & 0.5500 \\ 1.0 & 0.55 & -0.6475 \\ 0.0 & -0.95 & 0.3800 \end{pmatrix}. \tag{29}$$

Similarly, the controllability matrix for the subspace S_2 is

$$P_{c2} = \begin{pmatrix} 0.0 & 1.00 & 1.0200 \\ 1.0 & 1.02 & 0.0904 \\ 0.0 & -0.95 & -0.0665 \end{pmatrix}. \tag{30}$$

As the controllability matrices in all the three subspaces have a full rank of 3, we find that the matrices $(\tilde{A}_i, B)$ form controllable pairs. Hence, the linearised parts of the memristive MLC circuit are controllable. To achieve state feedback control, we assume a 'switched state feedback control law' [50],

$$u = \begin{cases} -\tilde{K}_2 x_0 & \text{if } x \in S_2, \\ -\tilde{K}_{1,3} x_0 & \text{if } x \in S_{1,3}, \end{cases} \tag{31}$$

where $\tilde{K}_i$'s are the 'control gain vectors' in the three subregions of the phase space and are found using the procedure outlined in the previous section as

$$\tilde{K}_2 = (-0.2050 \quad 0.8290 \quad -1.2300) \tag{32}$$

and

$$\tilde{K}_{1,3} = (0.5040 \quad 1.4825 \quad 2.0000). \tag{33}$$

The 'closed-loop system' for the memristive MLC circuit upon application of gain is

$$\dot{x}_0(t) = \begin{cases} (\tilde{A}_2 - B^T \tilde{K}_2) x_0 & \text{if } x \in S_2, \\ (\tilde{A}_{1,3} - B^T \tilde{K}_{1,3}) x_0 & \text{if } x \in S_{1,3}, \end{cases}$$
$$y = C_0^T x + D^T u. \tag{34}$$

As the eigenvalues of the matrices $(\tilde{A}_i - B^T \tilde{K}_i)$, $i = 1, 2, 3$ lie within the unit circle, the dynamics of the controlled closed system settles down to a non-chaotic equilibrium state. The chaotic attractor of the system before the application of the state feedback control and the controlled periodic state after the control has been applied are shown in figure 6.

The time series of the system which is chaotic before the application of control becomes periodic after the control is applied. This regulation of the chaotic time series to a periodic behaviour for the initial conditions $(x_1 = -0.1, x_2 = -0.1, x_3 = -0.1)$ is shown in figure 6a(i) while the periodic attractor in the (x_1-x_2) phase
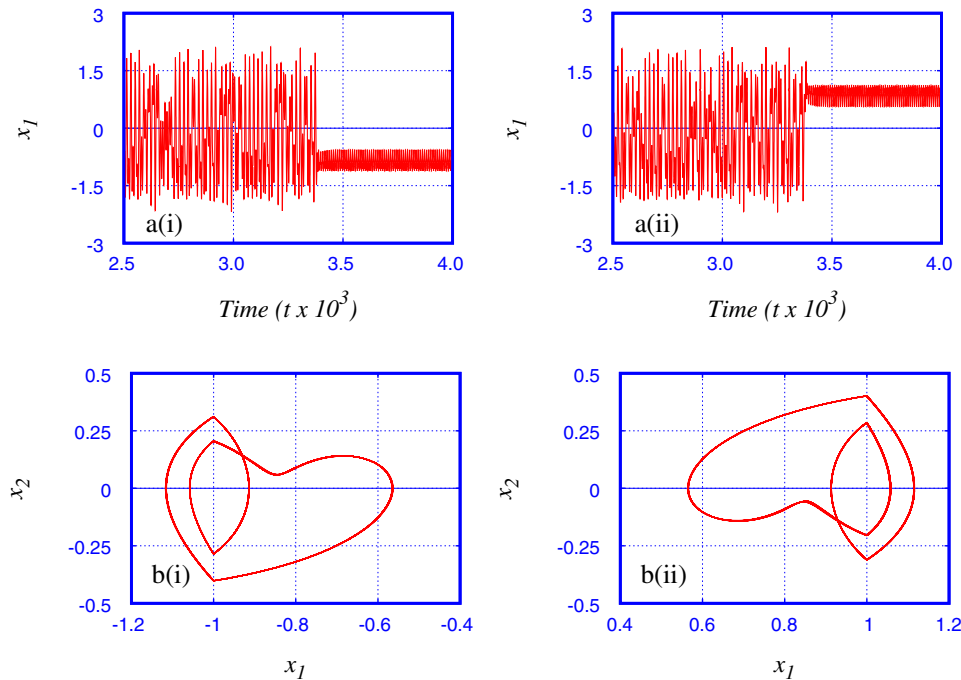
Figure 6. The periodic oscillations of the memristive MLC oscillator after the application of the state feedback control are shown in **a(i)** and **a(ii)** time plots and **b(i)** and **b(ii)** phase portraits in the (x_1–x_2) plane. A change in the initial conditions from $x_1 = -0.1, x_2 = -0.1, x_3 = -0.1$ to $x_1 = -0.2, x_2 = -0.2, x_3 = -0.2$ results in the symmetric interchange of the time plots and attractors about the origin. The step size is assumed as $h = \frac{1}{1000}(2\pi/\omega)$, with $\omega = 0.65$ and $f = 0.20$.

plane in the asymptotic limit is shown in figure 6b(i). However, if the initial conditions are changed to $x_1 = -0.2, x_2 = -0.2, x_3 = -0.2$, we observe an inversion of the time series for the variable x_1 and the periodic attractor in (x_1–x_2) phase space as are shown in the corresponding figures 6a(ii) and 6b(ii).

It is pertinent to state here that the memristive MLC system may possess multistability (see figures 3 and 6). This is because we see that in these two cases, a mere change in the initial conditions forces the system to exhibit different dynamics. If the system were to possess multistability, then we strongly believe that by tweaking the control gain vectors K_1 and K_2, it can be directed to take on any of the desired multistable states.

5. Synchronisation of chaos

The feasibility of synchronisation of chaotic systems and the conditions to be satisfied for the same were first demonstrated by Pecora and Caroll [54] by introducing the concept of drive–response systems. Here, a chaotic system is considered as the 'drive' system and a part of or subsystem of this drive system is considered as the 'response'. Under the right conditions (the conditional Lyapunov exponents (CLEs) of the error dynamics being negative), the signals of the

response part will converge to those of the drive system as time elapses. Ever since this ground breaking work, many researchers have proposed synchronisation of chaos in different systems based on theoretical analysis and even experimental realisations. For example, this methodology has been successfully applied to synchronise chaos in Lorenz systems [54–56], Rössler systems [54], the hysteretic circuits [57], Chua's circuits [58], driven Chua's circuits [59], Chua's and MLC circuits [60,61], ADVP oscillators [62,63], phase locked loops (PLL) [64,65], etc.

Further, the possibility of applying this approach for secure communication has been demonstrated. The idea of 'chaotic masking and modulation' and 'chaotic switching' for secure communication of information signals based on Pecora and Caroll method of synchronisation of chaos was demonstrated numerically by Cuomo and Oppenheim [66–69] and experimentally by Koracev *et al* [59] using Chua's circuit as the chaos generator. Further, the applicability of chaotic synchronisation to digital secure transmission was demonstrated in [66] and experimentally in [63,70]. The possibility of synchronisation of hyperchaotic systems and its applicability for communication purposes was proposed by Peng *et al* [71]. All these works make secure communications more practicable and with improved degree of security.

Many alternative schemes of synchronisation based on modifications of the drive–response concept, such as the unidirectional coupling scheme [62,63], function projective synchronisation [72], hybrid function projective synchronisation [73–77], the arbitrary hybrid function projective synchronisation [78–80] etc. have been proposed. The synchronisation of two canonical Chua's circuits using resistive unidirectional coupling has been studied by Thamilmaran and Senthilkumar [81] and two unidirectional coupled SC-CNN-based canonical Chua's circuits has been realised experimentally by Swathi *et al* [82]. The synchronisation and propagation of a low-frequency signal in a network of unidirectionally coupled Chua's circuits driven by a biharmonic external excitation has been studied by Jothimurugan *et al* [83]. However, all these methods have drawbacks such as,

1. they do not give a systematic procedure for determining the response system and the drive signal. This means that most of the schemes are dependent on the drive system and could not be generalised to an arbitrary drive system.
2. the dynamics of the drive system should be free of any disturbances.
3. the conditional Lyapunov exponents (CLEs) should be negative. This condition restricts the signal to be transmitted to be a small perturbation to the state variables. As this requirement is not fulfilled by non-smooth systems, such as in the case of a two-coupled memristive MLC system, effecting synchronisation should necessarily be obtained by other techniques only.

The concept of adaptive synchronisation is applied in [84–86] and observer-based approaches in [87,88] to overcome these difficulties of the drive–response concept.

6. Observer-based adaptive synchronisation of chaos

Let us consider the state-space representation of a SISO nonlinear system [42], defined in eq. (A.1) in Appendix A,

$$
\begin{aligned}
\dot{x} &= \tilde{A}x + B^T u, \\
y &= C^T x + D^T u,
\end{aligned}
\tag{35}
$$

where $\tilde{A} \in \mathcal{R}^{n \times n}$, $B \in \mathcal{R}^{n \times r}$, $C \in \mathcal{R}^{n \times l}$ and $D \in \mathcal{R}^{l \times r}$ are matrices, u is an r-dimensional vector denoting the control input and y is an l-dimensional vector representing the output of the system. The control input can be given as

$$
u = d + \theta^T f(x, y),
\tag{36}
$$

where $d \in R$ is a bounded disturbance, $\theta \in R^p$ is the constant parameter vector and $f(x, y)$ is a p-dimensional vector differential function.

When all the state variables of this system are unavailable for measurement, then according to the control theory, the states of the system may be estimated by designing a parametric model of the original system. This parametric model is called an 'observer' and is considered as the response system. The concept of observer design is a well-established branch of control engineering and is widely used in the state feedback control of dynamical systems [41,43,44]. In this method, once the drive system and its related observer are chosen, then under certain conditions, local or global synchronisation between the drive and the observer system is guaranteed [87].

Let us assume that the output $y(t)$ is the only variable that can be measured for the system (eq. (35)). Then an observer based on the available signal can be derived to estimate the state variables. This observer is known in the literature as the 'Luenberger observer' [42] and is given as

$$
\begin{aligned}
\dot{\hat{x}} &= \tilde{A}\hat{x} + L^T(y - \hat{y}) + B^T \hat{u}, \\
\hat{y} &= C^T \hat{x} + D^T \hat{u},
\end{aligned}
\tag{37}
$$

where $\hat{x}$ denotes the dynamic estimate of the state variable x, $L \in \mathcal{R}^n$ is an n-dimensional vector called the 'observer gain vector'. It is essential that eq. (37) is in observer canonical form, refer eq. (A.10) in Appendix A.

The control law can be derived as

$$
\hat{u} = \hat{d} + \hat{\theta}^T f(x, y),
\tag{38}
$$

where $\hat{d}$ and $\hat{\theta}$ are the estimates of the disturbances and the parameters of the system and are updated according to the adaptive algorithm [89] as

$$
\begin{aligned}
\dot{\hat{d}} &= (y - \hat{y}), \\
\dot{\hat{\theta}} &= f(x, y)(y - \hat{y}).
\end{aligned}
\tag{39}
$$

The Luenberger observer equations (37) have a feedback term that depends on the output observation error $\tilde{y} = y - \hat{y}$. Then the state observation error $\tilde{x} = x - \hat{x}$ satisfies the equation

$$
\begin{aligned}
\dot{\tilde{x}} &= (\tilde{A} - L^T C)\tilde{x} + B^T[(d - \hat{d}) + (\theta^T - \hat{\theta}^T)f(x, y)], \\
\tilde{x}(0) &= x_0 - \hat{x}_0,
\end{aligned}
\tag{40}
$$

where we assume $X = (\tilde{A} - L^T C)$ as the augmented system matrix. The implementation of this observer-based adaptive synchronisation of nonlinear systems is illustrated in figure 7.
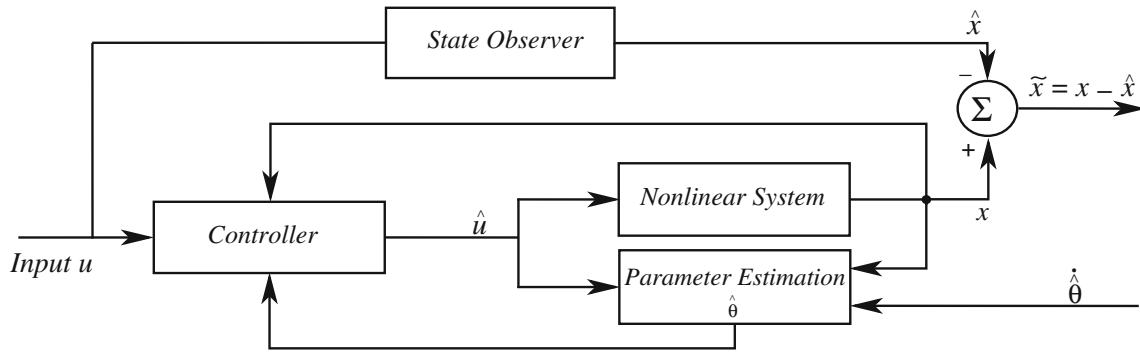
Figure 7. Block diagrammatic representation of the observer-based adaptive synchronisation of nonlinear systems.

6.1 *Conditions for stability*

According to control theory, the system represented by eq. (37) is stable in the sense of Lyapunov [42], refer §A.1 of Appendix A, if any of the following conditions are satisfied:

1. All eigenvalues of the augmented matrix $X = (\tilde{A} - L^T C)$ have negative real parts.
2. For every positive definite matrix Q (that is $Q = Q^T > 0$), the following Lyapunov matrix equation

$$X^T P + PX = -Q, \tag{41}$$

   has a unique solution P that is also positive definite.
3. For any given matrix C, with the pair (C, X) being observable, the equation

$$X^T P + PX = -C^T C, \tag{42}$$

   has a unique solution P, that is also positive definite.

If $(C^T, \tilde{A})$ is an observable pair, then we can choose the values of the gain vector L such that the matrix $(\tilde{A} - L^T C)$ is stable. In fact, the eigenvalues of the matrix $(\tilde{A} - L^T C)$, and therefore the rate of convergence of $\tilde{x}(t)$ to zero can be arbitrarily chosen by designing the vector L appropriately [41].

The observer-based response system given by eq. (37) and associated with the control law given by eq. (36) and the adaptive algorithm given by eq. (39) will now globally and asymptotically synchronise with the drive system given by eq. (35), that is

$$\|\tilde{x}(t)\| = \|x(t) - \hat{x}(t)\| \to 0 \text{ as } t \to \infty,$$

for all initial conditions.

Thus, we find that the adaptive synchronisation scheme is based on the following:

1. the linear part of the system is observable, that is the pair $(C^T, \tilde{A})$ is observable,

2. design of a suitable observer based on an adaptive law
3. formulation of a suitable control law.

7. Observer-based adaptive synchronisation of chaos in coupled memristive MLC oscillators

In this section, we report the synchronisation of chaos via an observer-based design, with appropriate control law and adaptive algorithm in a system of two-coupled memristive MLC circuits. As in the case of control of chaos, we assume that under appropriate choice of the boundary equilibrium points, the memristive MLC circuit becomes a Filippov system. Further, we assume the same parameter values as were fixed for effecting control in a single memristive MLC circuit, namely $a_{1,3} = -0.55$, $a_2 = -1.02$ and $\beta = 0.95$, $f = 0.20$ and $\omega = 0.65$. Also we assume the observer canonical form of the state-space representation of the memristive MLC circuit as given in eq. (23), namely

$$\dot{x}_0(t) = \begin{cases} \tilde{A}_2 x_0 + B^T u & \text{if } x \in S_2, \\ \tilde{A}_{1,3} x_0 + B^T u & \text{if } x \in S_{1,3}, \end{cases}$$

$$y = C^T x + D^T u, \tag{43}$$

where the system matrices $\tilde{A}_i$'s and the vectors B^T, C^T and D^T are the same as given in eqs (24)–(28). Then the observability matrices for the suspaces $S_{1,3}$ are

$$P_{0_{1,3}} = \begin{pmatrix} 1.00 & 0.00 & 0.00 \\ 0.00 & 1.00 & 0.00 \\ 0.00 & 0.55 & 1.00 \end{pmatrix}. \tag{44}$$

Similarly, the observability matrix for the subspace S_2 is

$$P_{0_2} = \begin{pmatrix} 1.00 & 0.00 & 0.00 \\ 0.00 & 1.00 & 0.00 \\ 0.00 & 1.02 & 1.00 \end{pmatrix}. \tag{45}$$

As these observability matrices in all the three subspaces have a full rank of 3, we find that the matrices (C^T, A_i) form an observable pair. Hence, the linearised parts of the memristive MLC circuit are observable. Under this condition, the Luenberger observer for the memristive MLC circuit can be derived as

$$\dot{\hat{x}}(t) = \begin{cases} \tilde{A}_2\hat{x} + L_2^T(y - \hat{y}) + B^T\hat{u} & \text{if } \hat{x} \in S_2, \\ \tilde{A}_{1,3}\hat{x} + L_{1,3}^T(y - \hat{y}) + B^T\hat{u} & \text{if } \hat{x} \in S_{1,3}, \end{cases}$$
$$\hat{y} = C^T\hat{x} + D^T\hat{u}, \tag{46}$$

where the control law is

$$\hat{u} = \hat{\theta}^T f(x, y), \tag{47}$$

with the vector $f(x, y)$ given as

$$f_1(x, y) = y,$$
$$f_2(x, y) = |y + 1| - |y - 1|, \tag{48}$$

is the differential function and $\hat{\theta}$ are the estimates of the parameters of the system and are updated according to the adaptive algorithm

$$\dot{\hat{\theta}}_1 = -(y - \hat{y})f_1(x, y),$$
$$\dot{\hat{\theta}}_2 = -(y - \hat{y})f_2(x, y). \tag{49}$$

The state error $\tilde{x} = \dot{x} - \dot{\hat{x}}$ dynamics is represented by

$$\dot{\tilde{x}} = \begin{cases} (\tilde{A}_2 - L_2^T C)\tilde{x} + B^T(\theta - \hat{\theta}^T)f(x, y), \\ (\tilde{A}_{1,3} - L_{1,3}^T C)\tilde{x} + B^T(\theta - \hat{\theta}^T)f(x, y). \end{cases} \tag{50}$$

The augmented matrices for the system can be defined as

$$X_i = (\tilde{A}_i - L_i^T C) \quad \text{for} \quad i = 1, 2, 3. \tag{51}$$

For the choice of parameters of the system mentioned above, the observer gain vectors L_i for each of the subspaces S_i are chosen so as to have the augmented matrices X_i to be exponentially stable.

For the subspaces $S_{1,3}$, the gain vectors are chosen as

$$L_{1,3} = (0.8000 \quad 3.1000 \quad -3.2870)^T. \tag{52}$$

Due to this choice of the observer gain vectors L_i, the augmented matrices $X_{1,3}$ in these subspaces $S_{1,3}$ will have poles at $\{0.0000, -0.6000 \pm i1.86748\}$. Similarly, for the subspace S_2, the gain vector is chosen as

$$L_2 = (0.0000 \quad 15.2212 \quad 13.6508)^T. \tag{53}$$

This will cause the augmented matrix X_2 to have poles at $\{-1.5788, 0.824398 \pm i4.13832\}$.

The Lyapunov equation for stability, eq. (41), may be written separately for the three subspaces as

$$X_i^T P_i + P_i X_i = -Q \quad \text{for} \quad i = 1, 2, 3, \tag{54}$$

where we assume matrix Q to be a three-dimensional unit matrix. The solutions of the above Lyapunov equation for stability for the subspaces $S_{1,3}$ are positive definite matrices $P_{1,3}$ given as

$$P_{1,3} = \begin{pmatrix} 1.7778 & -0.4220 & -0.7308 \\ -0.4220 & 2.7528 & -0.1558 \\ -0.7308 & -0.1558 & 0.6020 \end{pmatrix}. \tag{55}$$

The matrix P_2 for the subspace S_2 is given as

$$P_2 = \begin{pmatrix} -0.0012 & -0.0615 & -0.0647 \\ -0.0615 & -3.0924 & -3.2555 \\ -0.0647 & -3.2555 & -3.4268 \end{pmatrix} \times 10^6. \tag{56}$$

We find that the matrix P_2 for the subspace S_2 is not a solution of the Lyapunov equation, eq. (54). Therefore, the trajectories in this subspace should be, as per Lyapunov theory, unstable. Hence, the augmented matrix X_2 in region S_2 is also unstable. However, the combined effect of the dynamics in the outer two subspaces $S_{1,3}$ represented by the augmented matrices $X_{1,3}$ and the positive definite matrices $P_{1,3}$ will impress upon the system as a whole to become asymptotically stable and exhibit a bounded behaviour asymptotically. Further, as the conditions for the Lyapunov asymptotic stability, eq. (54), are satisfied by the system as a whole, we find that under the action of the control law, eq. (47), and the adaptive algorithm, eq. (49), the estimated values of the unknown parameters of the observer system $\hat{a}_i$'s converge finally to the true values of the parameters a_i's as time progresses. These are shown in figure 8, where we find that in figure 8a the value of the parameter $\hat{a}_2$ converges to its true value of -1.02, while in figure 8b the value of the parameter $\hat{a}_1$ converges to its true value of -0.55.

Mathematically we have the error between the drive and the response, converging to zero for all initial values, as time progresses, that is

$$\| \tilde{x}(t) \| = \| x(t) - \hat{x}(t) \| \rightarrow 0 \text{ as } t \rightarrow \infty.$$

The convergence of the error dynamics $\tilde{x}$ to zero is shown in figure 9. Here the convergence of the errors $\tilde{x}_1, \tilde{x}_2$ and $\tilde{x}_3$ are shown in plots (a), (b) and (c) of figure 9 respectively.

These convergences of the parameters to their true values and that of the error dynamics to zero, cause the observer system dynamics to converge to the original system dynamics as time elapses. This means that the response system dynamics evolves as time proceeds to that of the drive system dynamics. Hence, if the drive system is in a chaotic state, then the response system should also exhibit identical chaotic state. This is shown in figure 10.
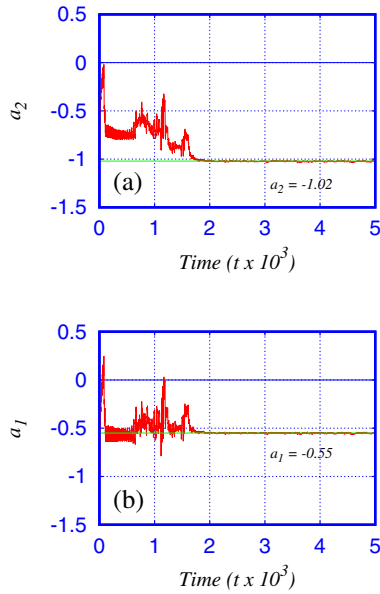
Figure 8. The estimation of (**a**) the parameter a_2 and (**b**) the parameter a_1 of the response system of the two-coupled memristive MLC circuit in the synchronised state using the adaptive observer scheme. It is to be noted that the asymptotic values of $a_2 = -1.02$ and $a_1 = -0.55$ are exactly equal to those of the drive system which were known *a priori*.

Had the drive system been in a periodic state, then one would expect the response system also to take on asymptotically the periodic state by virtue of the adaptive synchronisation. As both the drive and the response systems exhibit identical behaviour, they are said to be in complete synchronisation (CS) with each other. This is shown by the diagonal lines for the variables in the $(x_1–x_1')$, $(x_2–x_2')$ and $(x_3–x_3')$ phase planes in plots (a), (b) and (c) respectively in figure 11.

For effecting this, it is essential that the gain vectors L_i for all the subspaces S_i's are properly chosen. Due to the differences in the gain vectors in the three subregions of the phase space, this observer-based adaptive synchronisation is also referred to in literature as 'switched state feedback' method of adaptive synchronisation [50].

8. Conclusion

In this work, we have studied the control of chaos in an individual memristive MLC circuit as well as the synchronisation behaviour in a system of two-coupled memristive MLC circuits using state feedback control and observer-based adaptive control techniques respectively. To realise these objectives, we have considered the memristive MLC circuit as a Filippov system, a non-smooth system having the order of discontinuity one and have derived the discontinuity mapping corrections
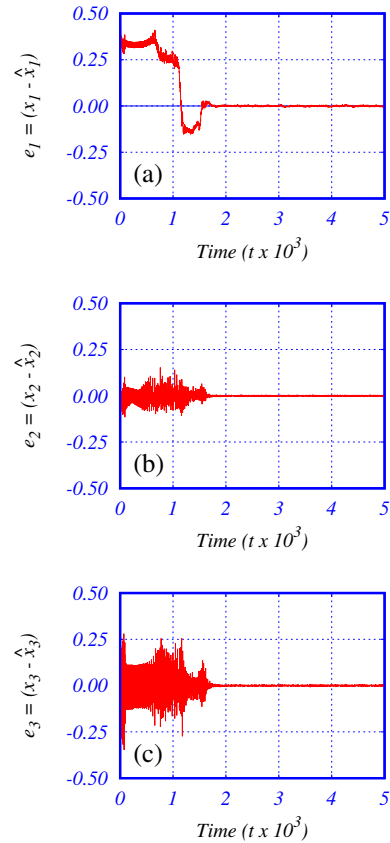

Figure 9. The convergences of the errors in the variables, (**a**) $e_1 = x_1 - x_1'$, (**b**) $e_2 = x_2 - x_2'$ and (**c**) $e_3 = x_3 - x_3'$ of the two-coupled memristive MLC circuit in the synchronised state under adaptive observer scheme.
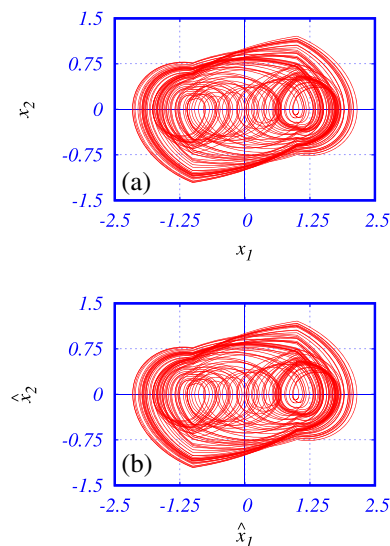

Figure 10. The phase portraits (**a**) in the $(x_1–x_2)$ plane and (**b**) in the $(\hat{x}_1–\hat{x}_2)$ plane showing identical chaos.
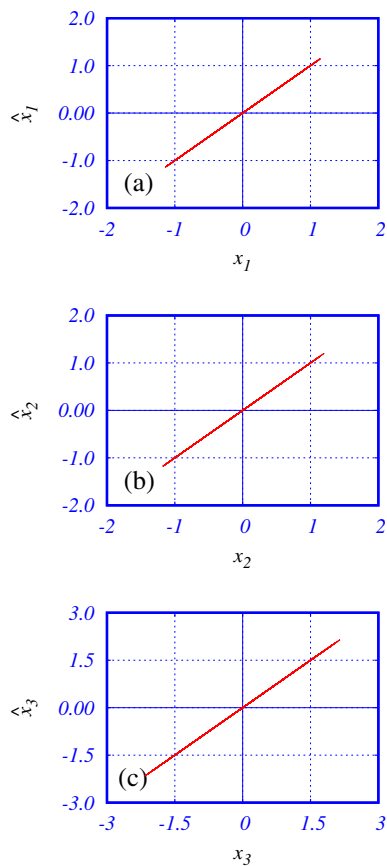
Figure 11. The complete synchronisation of the two-coupled memristive MLC circuit under the adaptive observer scheme in (**a**) (x_1-x_1') plane, (**b**) (x_2-x_2') plane and (**c**) (x_3-x_3') plane.

such as ZDM and PDM. Further, we have derived the canonical state-space representations for the memristive MLC circuit. Also the stability theory of Lyapunov and pole-placement methods, concepts which are very much familiar in control theory, were applied.

We wish to state here that we have derived analytical conditions for effecting control and adaptive synchronisation using state feedback and implemented the results using numerical simulations. The fact that the results of simulations agree with the predictions of the analytical conditions point to the validity of our derivations.

From a different point of view, it has been shown by many researchers, that in general any two coupled systems, be they smooth or discontinuous, can be directed towards amplitude death or oscillation death, irrespective of their being in periodic, chaotic, hyperchaotic or time-delay systems, by the application of proper feedback coupling, for example see [90]. The same can be applied to the two-coupled system under study, by calculating proper observer gain vectors and choosing proper initial conditions and parametric values. However, we have not proceeded along these lines because it falls

beyond the realm of this present work. We hope to pursue this possibility in future studies.

The phenomenon of control of chaos may be further studied to understand and effectively prevent incidences of nonlinear catastrophic phenomena such as blackouts in transmission lines and power grids, cardiac arrythmias, etc. The synchronisation of chaos which we have demonstrated using observer-based adaptive scheme in memristive MLC circuits can be used to effect digital modulation schemes for secure communication. For example, the modulation characteristics of the memristor can be used to implement amplitude shift keying (ASK), a key technique in digital signal processing and transmission of digitised information. Also the switching characteristics of the memristor can be utilised to implement digital protocols for secure transmission of data.

Acknowledgements

Appendix A. Space representations of dynamical systems

The state-space representation refers to the modelling of dynamical systems in terms of state vectors and matrices so that the analyses of such systems are made conveniently in the time domain, using the basic knowledge of matrix algebra. The main advantage of this approach is that it presents a uniform platform for representing time-varying as well as time-invariant systems, linear as well as piece-wise nonlinear systems. The theoretical details presented here are essentially from the available literature on control systems [41,42].

The generic state-space representation of an nth-order dynamical system is given as

$$\dot{x} = Ax + Bu,$$
$$y = C^T x + Du, \tag{A.1}$$

where x is an n-dimensional vector representing the state variables, $A \in \mathcal{R}^{n \times n}$, $B \in \mathcal{R}^{n \times r}$, $C \in \mathcal{R}^{n \times l}$ and $D \in \mathcal{R}^{l \times r}$ are matrices, u is an r-dimensional vector denoting the control input and y is an l-dimensional vector representing the output of the system.

The first of eq. (A.1) is referred to as the 'state equation' while the second is referred to as the 'output equation'. The solution of the state equation is given by

$$x(t) = e^{A(t-t_0)} x(t_0) + \int_{t_0}^{t} e^{A(t-\tau)} Bu(\tau) \, d\tau, \qquad \text{(A.2)}$$

where $e^{At} \equiv \Phi(t)$ is the state transition matrix and $x(t_0)$ is the initial state of the system.

1. *Open-loop system*: If the output of the system is neither fedback to the input nor is it used to modulate the behaviour of the system, then the system is called as an open-loop system.
2. *Closed-loop system*: If the output of the system is used to modulate the system and manipulate the control action on the system through some suitable feed-back mechanism, then the system is known as closed-loop system.
3. *Exponential stability*: An equilibrium state x_e is said to be exponentially stable, if there exists a constant $\alpha > 0$, and for every small constant $\epsilon > 0$ there exists a small neighbourhood $|x_0 - x_e| < \delta(\epsilon)$ such that

$$|x(t; t_0, x_0) - x_e| \leq \epsilon e^{-\alpha(t-t_0)}. \qquad \text{(A.3)}$$

Here α is called as the rate of convergence.

4. *Asymptotic stability*: An equilibrium state x_e is said to be asymptotically stable in the sense of Lyapunov [42] if any of the following conditions are satisfied:

   (a) All eigenvalues of the matrix A have negative real parts.
   (b) For every positive definite matrix Q (that is $Q = Q^T > 0$), the following Lyapunov matrix equation

   $$A^T P + PA = -Q, \qquad \text{(A.4)}$$

   has a unique solution P that is also positive definite.
   (c) For any given matrix C, with the pair (C^T, A) being observable, the equation

   $$A^T P + PA = -C^T C, \qquad \text{(A.5)}$$

   has a unique solution P, that is also positive definite.

5. *Observability*: It refers to the determination of the state of a system by observing or measuring its output. Mathematically, it is determined by finding the rank of the observability matrix

$$P_0 = \begin{pmatrix} C^T \\ C^T A \\ C^T A^2 \\ \vdots \\ C^T A^{n-1} \end{pmatrix}. \qquad \text{(A.6)}$$

The observability matrix is of dimension $n \times nl$. If this observability matrix has a full rank, equal to n, then the dynamical system or the pair (C^T, A) is said to be observable. However, if P_0 is an $n \times n$ square matrix, then the system is observable if P_0 is non-singular.

6. *Detectability*: A dynamical system may not be completely observable. However, if the unobservable parts of the system become asymptotically stable under the action of some control law, then the system is called as 'detectable' [41].
7. *Controllability*: It refers to the transferring of a system from any given initial state $x(t_0)$ to any given desired final state $x(t_f)$ over a finite interval of time $(t_f - t_0)$. Mathematically, it is determined by the rank of the controllability matrix

$$P_c = \begin{pmatrix} B \\ AB \\ A^2 B \\ \vdots \\ A^{n-1} B \end{pmatrix}.$$

The controllability matrix is of dimension $n \times nr$. If this controllability matrix has a full rank, equal to n, then the dynamical system or the pair (A, B) is said to be controllable. However, if P_c is an $n \times n$ square matrix, then the system is controllable if P_c is non-singular.

8. *Stabilizability*: A dynamical system may not be completely controllable. However, if the uncontrollable parts of the system become asymptotically stable under the action of some control law, then the system is called as 'stabilisable' [41].

A.1 *Forms of state-space representations*

For any given dynamical system, there are essentially an infinite number of possible state-space models that give identical input/output dynamics. However, it is often desirable to have certain standardised state-space model structures called the canonical forms or canonical state-space representations. Using similarity transformations, it is possible to convert the state-space model from one canonical form to another [41]. Two of the most important canonical forms in control theory are the observer canonical form and the controller canonical form.

A.1.1 *Observer canonical form*:
Let us consider the coordinate transformation $x_0 = Wx$, where $W = TP_0$ is a transformation matrix, P_0 is the observability matrix and the matrix T is constructed using the coefficients of the characteristic polynomial of the state matrix A.

$$T = \begin{pmatrix} 1 & 0 & 0 & \cdots & 0 \\ \tilde{a}_1 & 1 & 0 & \cdots & 0 \\ \tilde{a}_2 & \tilde{a}_1 & 1 & \cdots & 0 \\ \vdots & \vdots & \vdots & \cdots & \vdots \\ \tilde{a}_{n-1} & \tilde{a}_{n-2} & \cdots & \cdots & 1 \end{pmatrix}. \tag{A.7}$$

The characteristic polynomial $\{|sI - A|\}$ itself is given as

$$p(s) = s^n + \tilde{a}_1 s^{(n-1)} + \tilde{a}_2 s^{(n-2)} + \cdots + \tilde{a}_{(n-1)} s + \tilde{a}_n. \tag{A.8}$$

Using the inverse coordinate transformation $x = W^{-1} x_0$, eq. (A.1) can be transformed to the observer canonical form as

$$\dot{x}_0 = \tilde{A}_0 x_0 + B^T u,$$
$$y = C_0^T x_0 + D^T u, \tag{A.9}$$

where the state matrix A_0 is obtained by the similarity transformation $A_0 = WAW^{-1}$ and is given as

$$\tilde{A}_0 = \begin{pmatrix} -\tilde{a}_1 & 1 & 0 & \cdots & 0 \\ -\tilde{a}_2 & 0 & 1 & \cdots & 0 \\ \vdots & \vdots & \vdots & \cdots & \vdots \\ -\tilde{a}_{n-1} & 0 & 0 & \cdots & 1 \\ -\tilde{a}_n & 0 & 0 & \cdots & 0 \end{pmatrix} \tag{A.10}$$

and

$$C_0^T = C^T W^{-1}. \tag{A.11}$$

A.1.2 *Controller canonical form*: In this case, let us consider an alternate coordinate transformation $x_c = Mx$, where $M = TP_c$ is a transformation matrix, P_c is the controllability matrix and the matrix T is constructed using the coefficients of the characteristic polynomial of the state matrix A and is given in eq. (A.7).

Using the inverse coordinate transformation $x = M^{-1} x_c$, eq. (A.1) can now be transformed alternatively to the controller canonical form as

$$\dot{x}_c = \tilde{A}_c x_c + B^T u,$$
$$y = C_c^T x_c + D^T u, \tag{A.12}$$

where the state matrix A_c is obtained by the similarity transformation $A_c = MAM^{-1}$ and is given as

$$\tilde{A}_c = \begin{pmatrix} 0 & 1 & 0 & \cdots & 0 \\ 0 & 0 & 1 & \cdots & 0 \\ \vdots & \vdots & \vdots & \cdots & \vdots \\ 0 & 0 & 0 & \cdots & 1 \\ -\tilde{a}_1 & -\tilde{a}_2 & -\tilde{a}_3 & -\tilde{a}_{n-1} & -\tilde{a}_n \end{pmatrix} \tag{A.13}$$

and

$$C_c^T = C^T M^{-1}. \tag{A.14}$$

References

[1] J M Gonzaléz-Miranda, *Synchronisation and control of chaos: An introduction for scientists and engineers* (Imperial College Press, London, 2004)

[2] E Ott, C Grebogi and James A Yorke, *Phys. Rev. Lett.* **64**(**11**), 1196 (1990)

[3] S Rajasekar and M Lakshmanan, *Physica D* **67**, 282 (1993)

[4] S Boccaleti, C Grebogi, Y C Lai, H Mancini and D Maza, *Phys. Rep.* **329**, 103 (2000)

[5] M Lakshmanan and K Murali, *Chaos in nonlinear oscillators: Controlling and synchronization* (World Scientific, Singapore, 1996)

[6] M Lakshmanan and S Rajasekar, *Nonlinear dynamics: Integrability, chaos and patterns* (Springer, New Delhi, 2003)

[7] S Boccaleti, J Kurths, G Osipov, D L Valladares and C S Zhou, *Phys. Rep.* **366**, 1 (2002)

[8] Ahamed A Ishaq and M Lakshmanan, *Int. J. Bifurc. Chaos* **23**(**6**), 1350098 (2013)

[9] A Ishaq Ahamed, K Srinivasan, K Murali and M Lakshmanan, *Int. J. Bifurc. Chaos* **21**(**3**), 737 (2011)

[10] M Itoh and L O Chua, *Int. J. Bifurc. Chaos* **18**(**11**), 3183 (2008)

[11] A Ishaq Ahamed and M Lakshmanan, *Int. J. Bifurc. Chaos* **27**(**6**), 1730021 (2017)

[12] M I Feigin, *Forced oscillations in systems with discontinuous nonlinearities* (Nauka, Moscow, 1994)

[13] M di Bernado, K H Johansson and F Vasca, *Int. J. Bifurc. Chaos* **11**(**4**), 1121 (2001)

[14] P Kowalczyk and M di Bernado, On a novel class of bifurcations in hybrid dynamical systems – the case of relay feedback systems, in: *Proc. of Hybrid Systems Computation and Control* (Springer-Verlag, 2001) pp. 361–374

[15] M di Bernado, P Kowalczyk and A Nordmark, *Physica D* **170**, 175 (2002)

[16] M di Bernado, P Kowalczyk and A Nordmark, *Int. J. Bifurc. Chaos* **13**, 2935 (2003)

[17] A Ishaq Ahamed, *Nonsmooth bifurcations in certain piecewise continuous nonlinear circuits*. Ph.D. thesis (Bharathidasan University, Tiruchirappalli, India, 2016)

[18] B A Huberman and E Lumer, *IEEE Trans. Circuits Syst. CAS* **37**(**4**), 547 (1990)

[19] S Sinha, R Ramaswamy and J Subba Rao, *Physica D* **43**, 118 (1990)

[20] Y C Lai, M Ding and C Grebogi, *Phys. Rev. E* **47**(**1**), 86 (1993)

[21] T Tel, *J. Phys. A* **24**, L1359 (1991)

[22] Y C Lai, T Tel and C Grebogi, *Phys. Rev. E* **48**(**2**), 709 (1993)

[23] J Singer, Y-Z Wang and Haim H Bau, *Phys. Rev. Lett.* **66**(**9**), 1123 (1991)

[24] G Chen and X Dong, *Int. J. Bifurc. Chaos* **2**(**2**), 407 (1992)

[25] G Chen, *IEEE Trans. Circuits Syst. CAS* **40**(**11**), 829 (1993)

[26] R Lima and M Pettini, *Phys. Rev. A* **41**(**2**), 726 (1990)
[27] Y Liu and J R R Leite, *Phys. Lett A* **185**, 35 (1994)
[28] K Wisenfeld and B McNamara, *Phys. Rev. A* **33**(**1**), 629 (1986)
[29] P Bryant and K Wisenfeld, *Phys. Rev. A* **33**(**4**), 2525 (1986)
[30] Y Braiman and I Goldhirsch, *Phys. Rev. Lett.* **66**(**20**), 2545 (1991)
[31] E A Jackson and A Hubler, *Physica D* **44**, 407 (1990)
[32] E A Jackson, *Phys. Lett. A* **151**, 478 (1990)
[33] E A Jackson and A Kodogeorgiou, *Physica D* **54**, 253 (1991)
[34] E A Jackson and A Kodogeorgiou, *Physica D* **50**, 341 (1991)
[35] E A Jackson, *Phys. Rev. A* **44**(**8**), 4839 (1991)
[36] T Kapitaniak, *Chaos Solitons Fractals* **2**(**5**), 519 (1992)
[37] T Kapitaniak, L J Kocarev and L O Chua, *Int. J. Bifurc. Chaos* **3**(**2**), 459 (1993)
[38] K Pyragas, *Phys. Lett. A* **170**, 421 (1992)
[39] G Chen and X Dong, *IEEE Trans. Circuits Syst. CAS* **40**(**9**), 591 (1993)
[40] C Hwang, J Hsheh and R Lin, *CSF* **8**(**9**), 1507 (1997)
[41] T Kailath, *Linear systems* (Prentice Hall, Englewood Cliffs, New Jersey, 1980)
[42] P A Ioannou and J Sun, *Robust adaptive control* (Prentice Hall, Englewood Cliffs, New Jersey, 1996)
[43] C T Chen, *Intorduction to linear systems theory* (Holt, Rinehart and Winston Inc., New York, 1970)
[44] C A Desoer and M Vidyasagar, *Feedback systems: Input–output properties* (Academic Press Inc., New York, 1975)
[45] M T Yassen, *Appl. Math. Comput.* **135**(**1**), 113 (2003)
[46] T-L Liao, *Phys. Rev. E* **57**(**2**), 1604 (1998)
[47] H-T Yau, *Chaos Solitons Fractals* **22**(**2**), 341 (2004)
[48] J Sun and Y Zhang, *Phys. Lett. A* **306**, 306 (2003)
[49] M T Yassen, *Phys. Lett. A* **360**, 582 (2007)
[50] J Zhang, H Zhang and G Zhang, Controlling chaos in a memristor-based Chua's circuit, in: *Proceedings of the International Conference on Communications, Circuits and Systems* (Milpitas, CA, July 2009)
[51] H H C Iu, D S Yu, A L Fitch, V Sreeram and H Chen, *IEEE CAS.-I* **58**(**6**), 1337 (2011)
[52] Y Song, Y Shen and Y Chang, Chaos control of a memristor-based Chua's oscillator via backstepping method, in: *Proceedings of the International Conference on Information Science and Technology* (Nanjing, Jiangsu, China, March 2011)
[53] E Sontag, *Mathematical control theory: Deterministic finite dimensional systems* (Springer, Berlin, 1998)
[54] L M Pecora and T L Caroll, *Phys. Rev. Lett.* **64**(**8**), 821 (1990)
[55] L M Pecora and T L Caroll, *IEEE Trans. Circuits Syst. CAS* **40**(**10**), 646 (1993)
[56] R He and P G Vaidya, *Phys. Rev. A* **46**(**12**), 7387 (1992)
[57] L M Pecora and T L Caroll, *IEEE Trans. Ciruits Syst. CAS* **38**(**4**), 453 (1991)
[58] Leon O Chua, L Kocarev, K Eckert and M Itoh, *Int. J. Bifurc. Chaos* **2**(**3**), 705 (1992)
[59] L Kocarev, K S Halle, K Eckert, Leon O Chua and U Parlitz, *Int. J. Bifurc. Chaos* **2**(**3**), 709 (1992)
[60] K Murali, M Lakshmanan and L O Chua, *Int. J. Bifurc. Chaos* **5**(**2**), 563 (1995)
[61] K Murali and M Lakshmanan, *Int. J. Bifurc. Chaos* **7**(**2**), 415 (1997)
[62] K Murali and M Lakshmanan, *Phys. Rev. E* **48**(**3**), R1624(R) (1993)
[63] M Lakshmanan and K Murali, *Curr. Sci.* **67**(**12**), 989 (1994)
[64] T Endo and L O Chua, *Int. J. Bifurc. Chaos* **1**(**3**), 701 (1991)
[65] M De Sousa Veria, A J Lichtenberg and M A Liberman, *Int. J. Bifurc. Chaos* **1**(**3**), 691 (1991)
[66] K M Cuomo and A V Oppenheim, *Phys. Rev. Lett.* **71**(**8**), 65 (1993)
[67] K M Cuomo, A V Oppenheim and S H Strogatz, *IEEE Trans. Circuits Syst. CAS* **40**(**1**), 626 (1993)
[68] K M Cuomo, *Int. J. Bifurc. Chaos* **3**(**5**), 1327 (1993)
[69] K M Cuomo, *Int. J. Bifurc. Chaos* **4**(**3**), 727 (1994)
[70] U Parlitz, Leon O Chua, L Kocarev, K S Halle and A Shang, *Int. J. Bifurc. Chaos* **2**(**4**), 973 (1992)
[71] J H Peng, E J Ding and W Yang, *Phys. Rev. Lett.* **76**(**6**), 904 (1996)
[72] R Mainieri and J Rehacek, *Phys. Rev. Lett.* **82**(**15**), 3042 (1999)
[73] C Y Chee and D Xu, *Phys. Lett. A* **318**, 112 (2003)
[74] D Xu, *Phys. Rev. E* **63**(**1**), 027201 (2001)
[75] D Xu and C Y Chee, *Phys. Rev. E* **66**(**4**), 046218 (2002)
[76] G Grassi and D A Miller, *Chaos Solitons Fractals* **39**(**3**), 1246 (2009)
[77] G Grassi and D A Miller, *Int. J. Bifurc. Chaos* **17**(**4**), 1337 (2007)
[78] M Hu, Z Xu, R Zhang and A Hu, *Phys. Lett. A* **365**, 315 (2007)
[79] J Lu and Q Zhang, *Phys. Lett. A* **372**, 1416 (2008)
[80] M Hu, Z Xu, R Zhang and A Hu, *Phys. Lett. A* **361**, 231 (2007)
[81] K Thamilmaran and D V Senthilkumar, Dynamics of two coupled canonical Chua's circuits, in: *Proceedings of 2nd National Conference on Nonlinear Systems and Dynamics (NCNSD)* (Aligarh, 2005) pp. 45–48
[82] P S Swathi, S Sabarathinam, K Suresh and K Thamilmaran, *Nonlinear Dyn.* **78**, 1033 (2014)
[83] R Jothimurugan, K Thamilmaran, S Rajasekar and M A F Sanjuán, *Int. J. Bifurc. Chaos* **23**(**11**), 1350189 (2013)
[84] C W Wu, T Yang and L O Chua, *Int. J. Bifurc. Chaos* **6**(**3**), 455 (1996)
[85] M diBernado, *Int. J. Bifurc. Chaos* **6**(**3**), 557 (1996)
[86] T L Liao, *Chaos Solitons Fractals* **9**(**9**), 1555 (1998)
[87] O Morgul and E Solak, *Phys. Rev. E* **54**(**5**), 4803 (1996)
[88] O Morgul and E Solak, *Int. J. Bifurc. Chaos* **7**(**6**), 1307 (1997)
[89] T-L Liao and Shin-Hwa Tsai, *Chaos Solitons Fractals* **11**(**9**), 1387 (2000)
[90] V Resmi, G Ambika and R E Amritkar, *Phys. Rev. E* **84**(**4**), 046212 (2011)